

Received April 27, 2020, accepted May 24, 2020, date of publication May 27, 2020, date of current version June 10, 2020.

Digital Object Identifier 10.1109/ACCESS.2020.2998058

Reduced Dynamic Modeling for Heavy-Duty Hydraulic Manipulators With Multi-Closed-Loop Mechanisms

YI ZHANG^{1,2,3}, WENHUA DING^{1,4}, AND HUA DENG^{1,2}, (Member, IEEE)

¹School of Mechanical and Electrical Engineering, Central South University, Changsha 410083, China

²State Key Laboratory of High Performance and Complex Manufacturing, Changsha 410083, China

³College of Mechanical and Electrical Engineering, Changsha University, Changsha 410022, China

⁴Shenzhen Colibri Technologies Company Ltd., Shenzhen 518057, China

Corresponding authors: Wenhua Ding (dwh00@163.com) and Hua Deng (hdeng@csu.edu.cn)

This work was supported in part by the National Key Research and Development Project under Grant 2019YFC1511503, and in part by the China Postdoctoral Science Foundation under Grant 2019M652794.

ABSTRACT A reduced dynamic modeling approach is introduced to systematically establish explicit closed-form dynamic equations for the main motion system of a heavy-duty hydraulic manipulator with multi-closed-loop mechanisms. The harmonious combination of the reduced system dynamic method with Lagrangian formulation, the principle of virtual work and screw theory greatly reduces the tedious calculation and largely simplifies the derivation of explicit control-orientated closed-form dynamic equations for complex multi-closed-loop mechanisms. Only three coupled subsystems, two Jacobian matrices, and two Hessian matrices are involved, thereby greatly reducing the order and the complexity of the closed-form dynamic equations. In addition to calculating the two Jacobian matrices by screw theory, the two Hessian matrices are also calculated straightforwardly by screw theory, thereby avoiding the difficulty in obtaining Hessian matrices by differentiating the Jacobian matrices and simplifying the calculation of the two Hessian matrices. No parts of dynamic equations are neglected in the derivation of the dynamic model. Thus, the accurate dynamic motion equations for the main motion system are obtained concisely. The derived closed-form dynamic equations are explicit with respect to the system inputs, which facilitate dynamics analysis and controller design. The experiments on the main motion system of the heavy-duty hydraulic forging manipulator demonstrate the efficiency of the proposed approach.

INDEX TERMS Dynamic modeling, heavy-duty hydraulic manipulator, multi-closed-loop mechanism, reduced system dynamic method, screw theory.

I. INTRODUCTION

Hydraulic systems are widely used in the industry, especially in large machinery, because of their ability to handle large inertia and torque loads. Multi-closed-loop manipulators, such as a class of parallel manipulators [1]–[4], are characterized by high stiffness, high accuracy, and high payload-to-weight ratio [4]. Therefore, hydraulic multi-closed-loop manipulators, integrated hydraulic actuators with a complex multi-closed-loop mechanical structure, have found promising applications in many heavy-duty applications, such as excavators, forging manipulators, palletizing robots, parallel manipulators, and so on [5]–[8]. The complex multi-

closed-loop mechanical structure has multiple closed loops, mutually coupled loop constraints, and complex parameter relations. Specifically, when integrated with hydraulic actuator dynamics, the dynamic behaviors of these manipulators can be highly nonlinear and complicated, causing difficulties in the control of such systems. Due to the complex topological structure of multi-closed-loop robotic manipulators or parallel robots, the dynamic modeling problem of these robotic mechanical systems has received increasing attention over the past decades [1], [2], [9]–[12]. However, most existing dynamic models on the complex multi-closed-loop mechanism mainly aim to achieve its optimal design and performance analysis [11]–[14]. With respect to the real-time control of multi-closed-loop robotic manipulators, an ideal dynamic model should be simple, highly computational

The associate editor coordinating the review of this manuscript and approving it for publication was Nishant Unnikrishnan.

efficient, and accurate enough to represent the physical system. Moreover, the model should be suitable for the direct promotion or application of most model-based control methods developed in the field of robot research [15]–[17].

Numerous formulations can be used to obtain the closed-form dynamic equations for closed kinematic chains [15], [18]–[20], such as Newton–Euler method, Kane’s method, Lagrangian formulation, Gibbs–Appell formulation, and the principle of virtual work. The first one is the Newton–Euler method [15], [18]. A comprehensive calculation is involved in this approach to obtain the acceleration of every isolated link of a manipulator and all constraint forces and moments between the joints, although the internal forces and moments of interaction are useless for the control of the manipulator [15], [19]. The second one is the well-known Kane’s method [15], [21], [22]. In this method, Kane’s dynamical equations are obtained by letting the sum of the total generalized active force and the total generalized inertia force equal to zero for each generalized coordinate of the system. In this manner, “no-working” internal constraint forces will disappear automatically [15]. The concepts of partial angular velocity and partial velocity are introduced to obtain the generalized forces needed for Kane’s equations [15], [21]. To obtain efficient equations, the generalized speeds that are important in Kane’s equations should be selected optimally though the explicit form of Kane’s equations with generalized speeds cannot be directly perceived by dynamicists [22]. Moreover, undetermined multipliers must be eliminated to derive the explicit dynamic equations with respect to the independent coordinates for the dynamic modeling of parallel mechanisms. Although the method is efficient especially when the dimension of the constraint equations is large, the calculation of partial velocities and accelerations is inevitable and slightly tedious [15]. The third method is the Gibbs–Appell method [20], which is one of the least used dynamic principles for formulating explicit equations of the motion of a manipulator [23]. In this approach, a Gibbs function (energy of acceleration) is initially defined, and a set of independent quasi-velocities (linear combination of generalized velocities) is then selected. The dynamic motion equations are then obtained by taking the derivative of the Gibbs function with respect to quasi-acceleration and equalizing them with generalized forces [20], [24], [25]. This formulation has efficient computational complexity and does not need to eliminate the undetermined multipliers for nonholonomic constraints to derive the explicit dynamic equations for the dynamic modeling of a closed-chain robotic system [20], [26]. However, the Gibbs–Appell method is less advantageous and may be more labor-intensive than the Kane’s method [22].

The fourth method for formulating motion equations is the principle of virtual work, which can efficiently derive dynamic models of parallel mechanisms [15], [18], [27]–[29]. The principle of virtual work lets the external forces perform work with any virtual velocity equal to zero, by which all dynamic equations of isolated bodies are combined into one dynamic equation of the parallel manipulator [15], [29]. All

reaction forces and moments can be removed from the virtual work equation. However, the calculation of the acceleration of every body is inevitably demanded. Moreover, the method is not straightforward for the forward dynamics because the velocity transform between joint and task spaces is complicated [27], and only an implicit model of inverse dynamics can be provided [15], [30]. The last one is the well-known Lagrangian formulation [15], [19]. In this approach, a set of generalized coordinates are selected to describe the configuration of the system, and the Lagrange equation is then used to derive the motion equations [19]. Lagrangian formulation is more efficient than Newton–Euler formulation because all unwanted reaction forces and moments are removed at the outset [19]. This approach has achieved considerable success for serial or open-chain mechanisms because the Lagrange equation is simply expressed by the actuator variables [15]; thus, the explicit closed-loop dynamics can be obtained directly. However, for parallel manipulators or complex closed-chain mechanisms, deriving explicit motion equations becomes a challenge because of the numerous constraints involved. Although this problem may be simplified by introducing additional coordinates along with a set of Lagrange multipliers, the computational load will increase inevitably [19].

The motion equations derived by different formulations are equivalent for a complex closed-chain mechanism [20]. However, the derived motion equations have different forms and advantages. For deriving a control-orientated dynamic model, Lagrangian formulation is more advantageous because the explicit closed-loop dynamics without unwanted reaction forces and moments can be derived directly [8]. The Lagrangian dynamic equations for open-chain mechanisms are popular because well-established motion equations exist, and many control results have been developed for such mechanisms [8], [31], [32]. Most existing control strategies for robots or manipulators are designed based on Lagrange equations [32]–[36]. As a result, Lagrangian formulation is the best candidate to serve the controller design among many dynamic modeling methods. However, different from open-chain mechanisms, one problem that needs to be solved first for deriving Lagrangian dynamic equations of multi-closed-loop or parallel mechanisms suitable for controller design is how to avoid the computational load increased by the numerous constraints involved in a multi-closed chain mechanism.

The Lagrangian method can be directly adopted to obtain the standard motion equations of closed-loop robots with a simple structure. A simplified approximate model by neglecting some links’ motion must be used to develop a dynamic model-based control [37]. The simplification makes the dynamics come up against additional uncertainties. Furthermore, a robust controller is required to handle such uncertainties. Accuracy and robustness are known as dilemmas. Hence, when the accuracy of a system model cannot be guaranteed, additional difficulties are left to the controller design and further efforts must be made to ensure the control performance of the system.

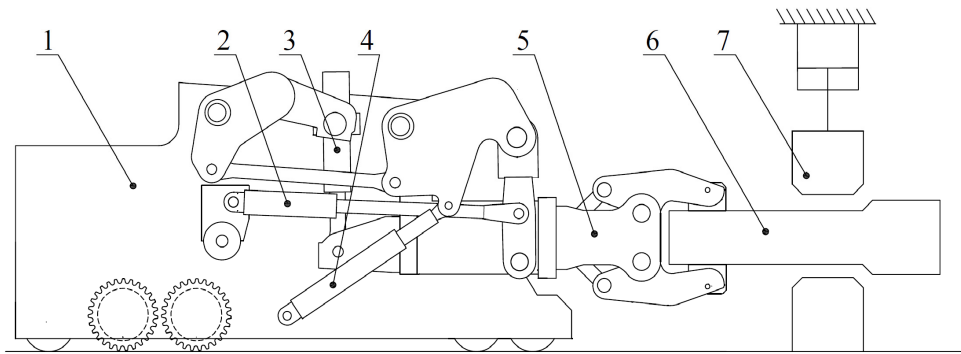


FIGURE 1. Diagram of a forging manipulator and a press machine (1-Truck frame; 2-Gripper feed cylinder; 3-Pitching cylinder; 4-Lifting Cylinder; 5-Gripper; 6-Forging workpiece; 7-Press machine).

In our previous work [8], the reduced system dynamic method [16], [38] was used to obtain standard Lagrangian formulations for the main motion system of a forging manipulator with multi-closed-loop mechanisms. The main motion system was divided into five serial mechanisms or simple subsystems with three Jacobian and three Hessian matrices. The Lagrangian equations were derived directly from the local generalized coordinates of each subsystem. D'Alembert principle was used to transform the generalized inputs with the local generalized coordinates of subsystems to the generalized forces with the generalized coordinates of the system by Jacobian matrices. The velocity and acceleration mapping between the local generalized coordinates of subsystems and the generalized coordinates were achieved by Jacobian and Hessian matrices. All Jacobian and Hessian matrices must be calculated among local generalized coordinates and generalized coordinates. Multi-closed-loop mechanisms are complex because of the geometric constraints caused by the multi-closed loop topology; thus, the calculation of the Jacobian and Hessian matrices of a complex mechanical system was difficult [8]. Screw theory was introduced to overcome the difficulties and simplify the calculation for solving kinematic and dynamic problems. However, only the three Jacobian matrices were calculated by screw theory, whereas the three Hessian matrices were calculated by differentiating the Jacobian matrices with Maple software [8], given that representing the acceleration in screw form is difficult [8], [39], [40]. The Hessian matrices were considerably more complicated than Jacobian matrices, and differentiating Jacobian was difficult because every element in the matrix is a complex implicit function about actuated pairs that consist of many passive pairs in this complex multi-closed-loop mechanism [8]. Each subsystem was described by a second-order differential equation. Merging the five subsystems could result in a high order and complicated dynamic model with a high computational cost for the main motion system of the hydraulic forging manipulator, causing difficulties in the controller design.

The dynamics of a parallel robot has also been solved based on the principle of virtual work and screw theory [29]. Similar with the method in [39], the Hessian matrix of the

parallel robot has been calculated by the intersection of all limbs' acceleration models in the traditional exponential matrix method [29]. However, the algorithms involved in the intersection are complicated, which can only be implemented by the force Jacobian matrix [3]. Few studies have considered the dynamic modeling of parallel manipulators or closed-chain mechanisms by using the combination of Kane's method and screw theory. For a knuckle boom crane with closed kinematic loops, its Kane's equations of motion are obtained by combining screw theory and the principle of virtual work [41]. In the knuckle boom crane, all the closed kinematic loops have a similar configuration with a two-link system actuated by a cylinder. An efficient and geometrically meaningful formulation can be obtained by the application of screw theory. However, the proposed approach in a study is specifically formulated for knuckle boom cranes and similar robotic manipulators [41].

Few theoretical studies on the calculation of Hessian matrices by using screw theory for a class of parallel manipulators have been conducted [3], [42]. In [3], [42], the Hessian matrix was formulated for a parallel robot with a fixed base and a moving platform and multi-lines with an identical structure. However, the formula is suitable for parallel robots [3] and may not be suitable for complex multi-closed-loop mechanisms. Therefore, further studies on the calculation of Hessian matrices by using screw theory for the main motion system of the forging manipulator with multi-closed-loop mechanisms are necessary.

In the present work, a reduced dynamic modeling approach is introduced to systematically establish explicit closed-form dynamic equations for a complex multi-closed-loop motion system of a heavy-duty hydraulic forging manipulator. First, the reduced system dynamic method is used to divide the multi-closed-loop mechanisms into several simple subchains. Second, the Lagrangian formulations are adopted to directly derive the explicit dynamic motion equations of each subchain. Third, the principle of virtual work with Jacobian and Hessian matrices is used to merge the subchain dynamic equations. Finally, screw theory is used to calculate the Jacobian and Hessian matrices. This approach has the

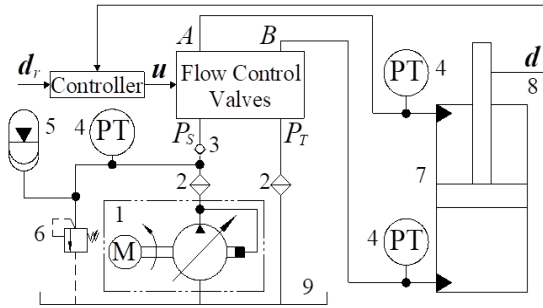


FIGURE 2. Hydraulic control system of the manipulator(1-Constant pressure pump; 2-Pressure filter; 3-Check valve; 4-Pressure transducer; 5-Accumulator; 6-Relief valve; 7-Hydraulic cylinder; 8-Position sensor; 9-Oil tank).

following five advantages. (1) The harmonious combination of the reduced system dynamic method with Lagrangian formulation, the principle of virtual work, and screw theory greatly reduces the tedious calculation and largely simplifies the derivation of explicit control-orientated closed-form dynamic equations. (2) The complex multi-closed-loop mechanisms are divided into three simply coupled subchains only. Thus, the motion equations for the main motion system are obtained with only two Jacobian and two Hessian matrices, thereby greatly reducing the order and decreasing system complexity. (3) In addition to calculating the two Jacobian matrices by screw theory [8], the two Hessian matrices are calculated straightforwardly by screw theory, thereby reducing the difficulty in differentiating Jacobian to obtain the Hessian matrices. (4) The accurate dynamic motion equations for the main motion system are obtained concisely without neglecting any part of the dynamic equations in deriving the dynamic model. (5) The derived closed-form dynamic equations for the main motion system with complex multi-closed-loop mechanisms are explicit with respect to the system inputs, that is, the valve spool position of practical hydraulic cylinders, which facilitate dynamics analysis and controller design. The experiments on the main motion system of a heavy-duty hydraulic forging manipulator demonstrate the efficiency of the proposed approach.

II. MODELING FOR THE MAIN MOTION SYSTEM OF THE HYDRAULIC MANIPULATOR

A. STRUCTURE DESCRIPTION

In general, a forging center should include a forging manipulator and a press machine, as shown in Fig. 1. The forging manipulator consists of a truck frame and an on-board multi-closed-loop mechanism, whose main task is to manipulate the forging workpieces [8]. The diagram of the multi-closed-loop robotic manipulator and its electro-hydraulic control system are illustrated in Figs. 1 and 2, respectively. The robotic manipulator is a 3-DOF multi-closed-loop mechanism, which is the key component of robotic manipulators and called the main motion mechanism. The whole construction enables movements of the gripper in two directions in a plane and its rotation about the axis normal to the plane, both of which

TABLE 1. Primary geometry parameters of the forging manipulator’s mechanism.

Parameter	Length	Parameter	Length
<i>GF</i> , <i>AB</i>	l_1	<i>DT</i>	l_7
<i>FD</i>	l_2	$\angle HGF$, $\angle IAB$	ϕ_4
<i>AG</i> , <i>HI</i> , <i>CD</i>	l_3	$\angle KGF$	ϕ_5
<i>FE</i>	l_4	<i>QK</i>	d_1
<i>GH</i> , <i>AI</i>	l_5	<i>LE</i>	d_2
<i>GK</i>	l_6	<i>BC</i>	d_3

achieve lifting, pitching, and horizontal feeding or buffering motions of the gripper. These motions are driven by three pairs of linear hydraulic actuators symmetrically assembled on the truck frame. Thus, the forging manipulator is a 3-DOF multi-closed loop mechanism. The electro-hydraulic system consists of several proportional directional flow control valves and a constant pressure variable displacement pump. The transfer of signals from a motion controller to proportional directional valves is conducted by a high-speed analog input module.

A geometric representation of the multi-closed-loop mechanism is displayed in Fig. 4. To facilitate the analysis, a based coordinate system $O - YZ$ is assigned at the point G of the truck frame with Z -axis along the vector from points A to B on the frame, and a moving coordinate system $P - yz$ is fixed at the point D of the gripper with z -axis along the vector from points C to D . The detail structure parameters of the links are shown in Table 1.

According to the working mode of a forging manipulator, the main function of pitching motion is to level the gripper, and the pitching cylinders are locked during the forging process. Thus, the pitching motion can be decoupled with two other main motions. Moreover, pitching motion is generally alone to save energy and deduce install power. Therefore, only two coupled motions, that is, lifting and horizontal feeding or buffering motions of the gripper, are considered. The pitching cylinder between points B and C , as displayed in Fig. 4, is locked in this study. In this case, only the dynamics of a two-DOF multi-closed-loop mechanism must be established because the pitching system is only a single DOF rotational mechanism.

B. RIGID BODY DYNAMICS FOR THE MAIN MOTION SYSTEM

To obtain a compact dynamic model for the main motion system with a structure similar to that of the open-chain manipulator, the reduced system dynamic method [8], [16], [38] is employed in this study.

C. MODELING OF AN OPEN-CHAIN REDUCED SYSTEM

Choosing a set of good independent generalized coordinates can simplify the derivation of the dynamic model and the

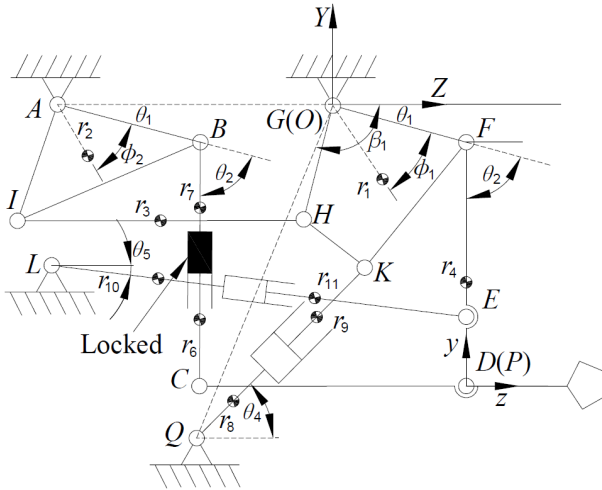


FIGURE 3. Geometric representation of the robotic mechanism.

calculation of the force transformation of Jacobian and Hessian matrices. Here, a set of independent generalized coordinates $q = [\theta_1 \ \theta_2]^T$ instead of linear actuators $d = [d_1 \ d_2]^T$ is chosen for modeling the dynamics. The multi-closed-loop mechanism, as shown in Fig. 4, is divided into three open-chain or simple mechanisms by cutting the complex multi-loop manipulator, as illustrated in Fig. 4.

Modules I–III in Fig. 4 resemble several serial robots or certain relative simple close-chain mechanisms. Generally, in the absence of friction and other disturbances, the standard Lagrangian formulation is an ideal choice and commonly used to derive the dynamic equations. The dynamic equations of Modules I–III are given as follows:

Module I:

$AIHG, ABFG$ and $BCDF$ are parallelogram. Therefore, Module I is equivalent to a 2-DOF R-P (R represents revolute pair, whereas P represents prismatic pair) planar mechanism, as shown in Fig. 3. Its dynamic model can be directly written as

$$M_1(q)\ddot{q} + C_1(q, \dot{q})\dot{q} + G_1(q) = \tau_1, \quad (1)$$

where $M_1(q_1) \in \mathbb{R}^{2 \times 2}$ denotes an inertia matrix, $C_1(q, \dot{q}) \in \mathbb{R}^{2 \times 1}$ is a vector that represents the Coriolis and centrifugal terms, $G_1(q) \in \mathbb{R}^{2 \times 1}$ represents a vector of the gravitational terms, and $\tau_1 = [\tau_{11} \ \tau_{12}]^T$ is a vector of generalized force.

Module II:

If generalized coordinates $q_2 = [\theta_4 \ d_1]^T$ are selected, Module II is a 2-DOF R-P planar mechanism, as illustrated in Fig. 3. Its dynamic model can also be obtained as

$$D_2(q_2)\ddot{q}_2 + \dot{q}_2^T H_{C_2}(q_2)\dot{q}_2 + g_2(q_2) = S_2, \quad (2)$$

where $D_2(q_2) \in \mathbb{R}^{2 \times 2}$ denotes an inertia matrix, $H_{C_2}(q_2) \in \mathbb{R}^{2 \times 2 \times 2}$ is a Hessian matrix related to the Coriolis and centrifugal terms, $g_2(q_2) \in \mathbb{R}^{2 \times 1}$ represents a vector of the gravitational terms, and $S_2 = [s_{11} \ s_{12}]^T$ is a vector of generalized force in the subsystem.

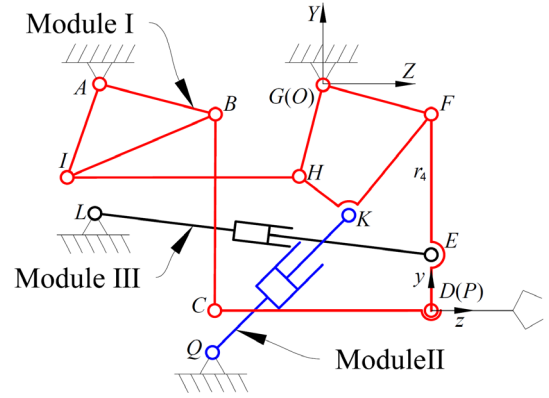


FIGURE 4. Reduced system model of the studied forging manipulator.

The parameters of M used for the inertia matrix in Equation (1) are defined by generalized coordinates, which are the position parameters d of hydraulic cylinders. However, the parameters of D in Equation (2) are the intermediate parameters of mechanisms, not the position parameters d of hydraulic cylinders.

If kinematic mapping can be solved between locally generalized coordinates q_2 and q , then the following equations can be used:

Velocity mapping:

$$\dot{q}_2 = J_2(q_2, q)\dot{q}, \quad (3)$$

Acceleration mapping:

$$\ddot{q}_2 = J_2(q_2, q)\ddot{q} + \dot{q}^T H_2(q_2, q)\dot{q}, \quad (4)$$

where $J_2(q_2, q) \in \mathbb{R}^{2 \times 2}$ denotes a kinematic Jacobian matrix, and $H_2(q_2, q) \in \mathbb{R}^{2 \times 2 \times 2}$ is a kinematic Hessian matrix.

According to the principle of virtual work, Equation (2) can be interpreted into generalized coordinates $q = [\theta_1 \ \theta_2]^T$ as

$$\tau_2 = J_2^T(q_2, q)S_2. \quad (5)$$

Substituting (3) and (4) into (2) and then combining (2) and (5) lead to

$$M_2(q_2, q)\ddot{q}_2 + C_2(q_2, q, \dot{q})\dot{q}_2 + G_2(q_2, q) = \tau_2, \quad (6)$$

where

$$M_2(q_2, q) = J_2^T(q_2, q)D_2(q_2)J_2(q_2, q);$$

$$C_2(q_2, q, \dot{q}) = \dot{q}^T \begin{bmatrix} J_2^T(q_2, q)D_2(q_2)^*H_2(q_2, q) \\ +J_2^T(q_2, q)J_2^T(q_2, q) \\ *H_{C_2}(q_2)J_2(q_2, q) \end{bmatrix};$$

$$G_2(q) = J_2^T(q_2, q)g_2(q_2);$$

$$\tau_2 = [\tau_{21} \ \tau_{22}]^T;$$

$$d_1 = \left[(y_Q + l_6 \sin(\theta_1 + \phi_5))^2 + (z_Q - l_6 \cos(\theta_1 + \phi_5))^2 \right]^{1/2}$$

$$\theta_4 = -\arcsin\left(\frac{y_Q + l_6 \sin(\theta_1 + \phi_5)}{d_1}\right).$$

The sign “*” denotes a generalized scalar product [43]. That of matrices $P \in \mathfrak{R}^{m \times n}$ and $Q \in \mathfrak{R}^{n' \times n' \times n'}$ can be defined as follows:

$$[P^*Q]_{k::} = \sum_{l=1}^n P_{k:l} Q_l \in \mathfrak{R}^{n \times n} \quad k = 1, 2, \dots, m, \quad (7)$$

where $P^*Q \in \mathfrak{R}^{m \times n}$, $P_{k:l}$ denotes the element on the k^{th} row and l^{th} column of matrix Q .

Module III:

Lifting and horizontal feeding hydraulic linear actuators may be regarded as the same modular because they have a similar structure, which is an R-P planar mechanism. Thus, the derivation of its dynamic model is similar with that of Module III. The dynamic model with local generalized coordinates $q_3 = [\theta_5 \ d_2]^T$ can be represented as follows:

$$D_3(q_3)\ddot{q}_3 + \dot{q}_3^T H_{C_3}(q_3)\dot{q}_3 + g_3(q_3) = S_3. \quad (8)$$

Velocity mapping:

$$\dot{q}_3 = J_3(q_3, q)\dot{q}, \quad (9)$$

Acceleration mapping:

$$\ddot{q}_3 = J_3(q_3, q)\ddot{q} + \dot{q}^T H_3(q_3, q)\dot{q}, \quad (10)$$

Similarly to Equation (5), $\tau_3 = J_3^T(q_3, q)S_3$. Then, the dynamic model of Module III can be written as

$$M_3(q_3, q)\ddot{q} + C_3(q_3, q, \dot{q})\dot{q} + G_3(q_3, q) = \tau_3, \quad (11)$$

where

$$\begin{aligned} M_3(q_3, q) &= J_3^T(q_3, q)D_3(q_3)J_3(q_3, q); \\ C_3(q_3, q, \dot{q}) &= \dot{q}^T \left[J_3^T(q_3, q)D_3(q_3)^*H_3(q_3, q) + J_3^T(q_3, q)J_3^T(q_3, q)^*H_{C_3}(q_3)J_3(q_3, q) \right]; \\ G_3(q) &= J_3^T(q_3, q)g_3(q_3); \\ \tau_3 &= [\tau_{31} \ \tau_{32}]^T; \\ d_2 &= \left[(-l_1 \sin \theta_1 - l_4 \sin(\theta_1 + \theta_2) - y_L)^2 + (l_1 \cos \theta_1 - l_4 \cos(\theta_1 + \theta_2) - z_L)^2 \right]^{1/2}; \\ \theta_5 &= \arcsin \left(\frac{y_L + l_1 \sin \theta_1 + l_4 \sin(\theta_1 + \theta_2)}{d_2} \right). \end{aligned}$$

The elements of all matrices or vectors in Modules I–III are given in Appendix A.

D. MODELING OF AN OPEN-CHAIN REDUCED SYSTEM

Combining (1), (6), and (11), the following equation can be obtained as

$$M(q_2, q_3, q)\ddot{q} + C(q_2, q_3, q, \dot{q})\dot{q} + G(q_2, q_3, q) = \tau, \quad (12)$$

where

$$M(q_2, q_3, q) = \sum_{i=1}^3 M_i C(q_2, q_3, q, \dot{q}) = \sum_{i=1}^3 C_i$$

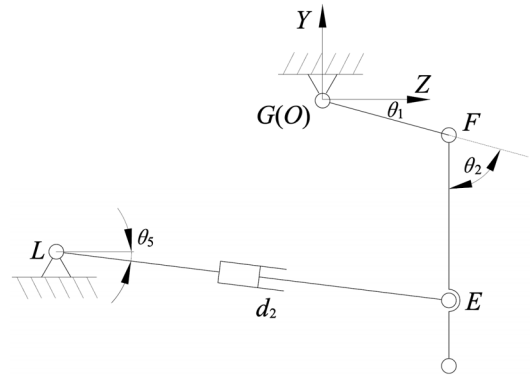


FIGURE 5. Closed-chain mechanism of the studied forging manipulator.

$$G(q_2, q_3, q) = \sum_{i=1}^3 C_i \quad \tau = \sum_{i=1}^3 \tau_i = [\tau_1 \ \tau_2]^T.$$

Likewise, the above equations based on generalized coordinate q can also be represented by the two pairs of linear actuator d . The velocity and acceleration mapping between q and d is as follows:

Velocity mapping:

$$\dot{d} = J(q, d)\dot{q} \quad (13)$$

Acceleration mapping:

$$\ddot{d} = J(q, d)\ddot{q} + \dot{q}^T H(q, d)\dot{q}, \quad (14)$$

Therefore, the dynamic model of the whole mechanism can be obtained as

$$D(q_2, q_3, q, d)\ddot{d} + C(q_2, q_3, q, d, \dot{d})\dot{d} + G(q_2, q_3, q, d) = f \quad (15)$$

where

$$\begin{aligned} D(q_2, q_3, q, d) &= [J^{-1}]^T M(q_2, q_3, q) J^{-1} \\ C(q_2, q_3, q, d, \dot{d}) &= \begin{bmatrix} \dot{d}^T [J^{-1}]^T [J^{-1}]^T * H(q_2, q_3, q, \dot{q}) J^{-1} \\ -\dot{d}^T [J^{-1}]^T M(q_2, q_3, q) J^{-1} * H_{d\theta} \end{bmatrix} \\ G(q_2, q_3, q, d) &= [J^{-1}]^T G(q_2, q_3, q, d) \\ f &= [f_1 \ f_2]^T \end{aligned}$$

is the driving force vector of the two pairs of hydraulic cylinders.

Equation (15) shows the input–output equations of velocity and acceleration for the main motion system with multi-closed-loop mechanisms, which are obtained by the standard Lagrangian formulation popular for the modeling of open-chain mechanical systems. As only three coupled subsystems with two Jacobian matrices and two Hessian matrices are involved, the complexity of the closed-form dynamic equations is greatly decreased.

III. FORMULATION OF THE HESSIAN MATRICES BASED ON SCREW THEORY

Screw theory is introduced to solve the Hessian matrices or second-order influenced coefficient matrices, making the derived standard Lagrangian equations of multi-closed-loop mechanisms based on the reduced system dynamic method concise. As previously mentioned, multi-closed-loop mechanisms are decomposed into three subsystems with several serial mechanisms by cutting certain joints. Thus, the Jacobian and Hessian matrices play an important role in constructing the dynamic model of multi-closed-loop mechanisms from the subsystems. In [8], screw theory was used to calculate the Jacobian matrices. However, the Hessian matrices were still obtained by differentiating the Jacobian matrices. In the present study, screw theory is used to cope with the problem of solving Hessian matrices for forming a harmonious combination between screw theory and reduced system dynamic method.

Hessian matrices, $\mathbf{H}_i(\mathbf{q}_i, \mathbf{q})$, should be calculated. Thus, only $\mathbf{H}_3(\mathbf{q}_3, \mathbf{q})$ is taken as an example to show how to calculate the Hessian matrices by using screw theory. In the closed-chain mechanism *GFEL*, two serial mechanisms can be obtained by cutting joint *E*, as shown in Fig. 5.

Serial mechanism *GFE* is 2-R mechanism that consists of two revolute pairs. The velocity state of point *E* in body *FE* with respect to the base coordinate system *O*–*YZ* is expressed as

$${}^0V_E = \mathbf{J}_3^{(1)} \dot{\mathbf{q}}, \quad (16)$$

where ${}^0V_E = \begin{bmatrix} v_x^{(E)} & v_y^{(E)} & v_z^{(E)} \end{bmatrix}^T \in \mathfrak{R}^{3 \times 1}$ is the linear velocity of the chosen reference point *E*; $\mathbf{J}_3^{(1)} = [\mathbf{G}_\varphi^P] \in \mathfrak{R}^{3 \times 2}$ is the Jacobian matrix of the serial mechanism, and given that the serial mechanism has two degrees of freedom, the Jacobian matrix has two columns; $[\mathbf{G}_\varphi^P]$ is given in Appendix B, which can be obtained by looking up Table 2 [42], [44]. $\dot{\mathbf{q}} = [\dot{\theta}_1 \ \dot{\theta}_2]^T$.

Similarly, the acceleration state of point *E* in body *FE* with respect to the base coordinate system *O* – *YZ* is expressed as

$${}^0A_E = \mathbf{J}_3^{(1)} \ddot{\mathbf{q}} + \dot{\mathbf{q}}^T \mathbf{H}_3^{(1)} \dot{\mathbf{q}}, \quad (17)$$

where ${}^0A_E = \begin{bmatrix} \ddot{v}_x^{(E)} & \ddot{v}_y^{(E)} & \ddot{v}_z^{(E)} \end{bmatrix}^T \in \mathfrak{R}^{3 \times 1}$ is the linear acceleration of the chosen reference point *E*; $\mathbf{H}_3^{(1)} = [\mathbf{H}_\varphi^P] \in \mathfrak{R}^{3 \times 3 \times 2}$ denotes the Hessian matrix for the serial mechanism. It is a three-dimensional vector with three layers, and each layer is a 3×2 matrix; $\mathbf{H}_3^{(1)}$ is given in Appendix B, which can be obtained by looking up Table 2 [42], [44].

Considering that the serial mechanism is a planar mechanism, the velocity competent along *X*-axis is zero, which is $v_x^{(E)} = \dot{v}_x^{(E)} = 0$. $\mathbf{J}_3^{(1)}$ should be a 2×2 matrix; $\mathbf{H}_3^{(1)}$ must be a $2 \times 2 \times 2$ matrix. Equation (17) can be simplified as

$$\mathbf{A}_E = \mathbf{J}_E^{(1)} \ddot{\mathbf{q}} + \dot{\mathbf{q}}^T \mathbf{H}_E^{(1)} \dot{\mathbf{q}}, \quad (18)$$

where $\mathbf{A}_E = \begin{bmatrix} \dot{v}_y^{(E)} & \dot{v}_z^{(E)} \end{bmatrix}^T \in \mathfrak{R}^{2 \times 1}$, $\mathbf{J}_E^{(1)} \in \mathfrak{R}^{2 \times 2}$ is a Jacobian matrix, and $\mathbf{H}_E^{(1)} \in \mathfrak{R}^{2 \times 2 \times 2}$ is a Hessian matrix constructed from matrices $\mathbf{H}_3^{(1)}$.

Equation (18) expresses the forward kinematics that can facilitate the formulation of the Hessian matrices by screw theory.

Likewise, the serial mechanism *LE* is an R-P mechanism and consists of two revolute pairs. The velocity and acceleration state of point *E* in body *LE* with respect to the base coordinate system *O* – *YZ* is expressed as

$${}^0V^E = \mathbf{J}_3^{(3)} \dot{\mathbf{q}}_3, \quad (19)$$

$${}^0A_E = \mathbf{J}_3^{(3)} \ddot{\mathbf{q}}_3 + \dot{\mathbf{q}}_3^T \mathbf{H}_3^{(3)} \dot{\mathbf{q}}_3, \quad (20)$$

$$\mathbf{A}_E = \mathbf{J}_E^{(3)} \ddot{\mathbf{q}}_3 + \dot{\mathbf{q}}_3^T \mathbf{H}_E^{(3)} \dot{\mathbf{q}}_3, \quad (21)$$

where $\mathbf{J}_3^{(3)} \in \mathfrak{R}^{3 \times 2}$ is the Jacobian matrix of serial mechanism *LE*, as shown in Appendix B; $\mathbf{H}_3^{(3)} = [\mathbf{H}_P] \in \mathfrak{R}^{3 \times 2 \times 3}$ denotes the Hessian matrix for the serial mechanism, as presented in Appendix B; $\dot{\mathbf{q}}_3 = [\dot{\theta}_5 \ \dot{d}_2]^T$, and $\ddot{\mathbf{q}}_3 = [\ddot{\theta}_5 \ \ddot{d}_2]^T$; $\mathbf{J}_E^{(3)} \in \mathfrak{R}^{2 \times 2}$ is a Jacobian matrix; $\mathbf{H}_E^{(3)} \in \mathfrak{R}^{2 \times 2 \times 2}$ is a Hessian matrix.

Given that the linear velocities of the chosen reference point *E* are equal, the following equations can be obtained from Equations (16), (18), (19), and (21).

$$\mathbf{J}_E^{(1)} \dot{\mathbf{q}} = \mathbf{J}_E^{(3)} \dot{\mathbf{q}}_3. \quad (22)$$

If matrix $\mathbf{J}_E^{(3)}$ is invertible, then the following equation can be obtained from Equation (22), which is the force transformation Jacobian matrix of Module III.

$$\dot{\mathbf{q}}_3 = \mathbf{J}_3(\mathbf{q}_3, \mathbf{q}) \dot{\mathbf{q}}. \quad (23)$$

Considering that the linear accelerations of the chosen reference point *E* are equal, the following equations can be obtained from Equations (17) and (20).

$$\mathbf{J}_E^{(3)} \ddot{\mathbf{q}}_3 = \mathbf{J}_E^{(1)} \ddot{\mathbf{q}} + \dot{\mathbf{q}}^T \mathbf{H}_E^{(1)} \dot{\mathbf{q}} - \dot{\mathbf{q}}_3^T \mathbf{H}_E^{(3)} \dot{\mathbf{q}}_3. \quad (24)$$

Substituting Equation (23) into Equation (24), the following is obtained:

$$\ddot{\mathbf{q}} = \mathbf{J}_3(\mathbf{q}_3, \mathbf{q}) \ddot{\mathbf{q}} + \dot{\mathbf{q}}^T \left(\mathbf{H}_E^{(1)} - [\mathbf{J}_3(\mathbf{q}_3, \mathbf{q})]^T \mathbf{H}_E^{(3)} \mathbf{J}_3(\mathbf{q}_3, \mathbf{q}) \right) \dot{\mathbf{q}} \quad (25)$$

Comparing Equation (25) with Equation (10), the following is obtained:

$$\mathbf{H}_3(\mathbf{q}_3, \mathbf{q}) = \mathbf{H}_3^{(1)} - [\mathbf{J}_3(\mathbf{q}_3, \mathbf{q})]^T \mathbf{H}_3^{(3)} \mathbf{J}_3(\mathbf{q}_3, \mathbf{q}) \quad (26)$$

Similarly, $\mathbf{H}_2(\mathbf{q}_2, \mathbf{q})$ can be calculated by screw theory in the above procedure, and the elements of the Jacobian and Hessian matrices are given in Appendix C. Thus, the two Hessian matrices are formulated by screw theory in a concise manner, other than by differentiating the Jacobian matrices.

In table 2, R and P represent revolute and prismatic pairs, respectively. S_n is a unit vector along the *n*th joint axis, P is a fixed point in link *j*, and R_n is a vector to the origin of the moving coordinate frame associated with joint *n*.

TABLE 2. Kinematic influence coefficients for serial manipulators.

Symbol	Joint type: n	Restriction	Value	
Translational first-order influence coefficients				
$[G_\varphi^P]_n$	R	$n \leq j$	$S_n \times (P - R_n)$	
	P	$n \leq j$	S_n	
	--			
Translational second-order influence coefficients				
$[H_\varphi^P]_{m:n}$	R	R	$m \leq n \leq j$	$S_m \times [S_n \times (P - R_n)]$
	R	R	$n < m \leq j$	$S_n \times [S_m \times (P - R_m)]$
	P	R	$m < n \leq j$	0
	P	R	$n < m \leq j$	$S_n \times S_m$
	R	P	$m < n \leq j$	$S_m \times S_n$
	R	P	$n < m \leq j$	0
	--	--	$(m \text{ or } n) > j$	0
	P	P	all m, n	0

IV. EXPLICIT CLOSED-FORM DYNAMIC EQUATIONS WITH HYDRAULIC SYSTEM DYNAMICS

The main motion system is driven by hydraulic systems, one of which is shown in Fig. 3, comprising a single-rod cylinder with a position sensor, a flow control valve, and a controller. To meet the demands of heavy-duty tasks, the large flow rate cartridge valves or the combine flow control valves are adopted to control the fluid in the class of hydraulic systems. An electric proportional pressure compensated flow control valve, as illustrated in Fig. 6, is also used to improve the speed control accuracy under varying loads [45].

By neglecting the main valve spool dynamics, control flows Q_{1i} and Q_{2i} can be described as [17], [46], [47]

$$\begin{cases} Q_{1i} = g_{1i}(x_{vi}) \sqrt{\frac{2}{\rho}} [s(x_{vi}) \sqrt{P_{mi} - P_{1i}} + s(-x_{vi}) \sqrt{P_{1i} - P_T}] \\ Q_{2i} = g_{2i}(x_{vi}) \sqrt{\frac{2}{\rho}} [s(x_{vi}) \sqrt{P_{2i} - P_T} + s(-x_{vi}) \sqrt{P_{mi} - P_{2i}}] \end{cases} \quad (27)$$

where x_{vi} is the valve spool position, and

$$s^{(*)} = \begin{cases} 1, & \text{if } * \geq 0 \\ 0, & \text{if } * < 0 \end{cases} \quad (28)$$

By neglecting the valve spool dynamics of the pressure compensated valve due to the low working frequency of the heavy-duty hydraulic forging manipulator, the following is obtained:

$$\begin{cases} P_{mi} - P_{1i} = \Delta P & \text{if } x_v \geq 0 \\ P_{mi} - P_{2i} = \Delta P & \text{if } x_v < 0 \end{cases} \quad (29)$$

where P_{mi} is the intermediate pressure after the pressure compensation valve, P_T is the tank pressure, and ΔP is the approximate constant across the adjustable orifice [45].

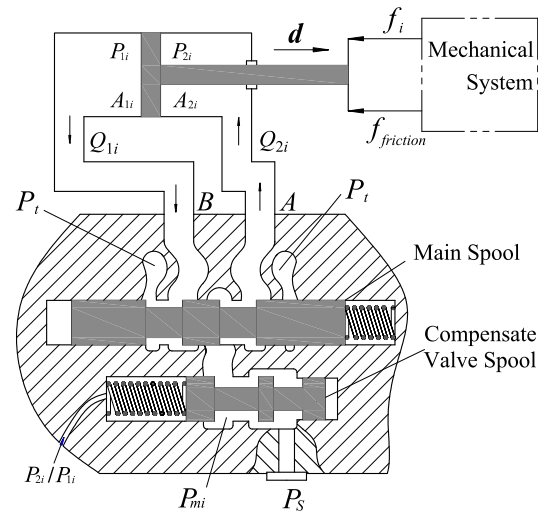


FIGURE 6. Diagram of a valve-controlled asymmetrical hydraulic cylinder.

For ideal servo valves, $g_{1i}(x_{vi})$ and $g_{2i}(x_{vi})$ are usually linear functions of the input signal u_i when the valve spool dynamics are disregarded. However, for cartridge valves or pressure compensated flow control valves applied in heavy-duty fields, their valve structures make the two functions non-linear [48]. Experiments show that the two functions can be approximated by high-order polynomials of the input signal u_i [17], which can be used in Equation (27) in this study.

By disregarding the external leakage, the oil flow continuity equations of the cylinder can be described as [17]

$$\begin{cases} A_{1i} \dot{d}_i + C_{ii} (P_{1i} - P_{2i}) + \frac{V_{01i} + A_{1i} d_i}{\beta_e} \dot{P}_{1i} = Q_{1i} \\ A_{2i} \dot{d}_i + C_{ii} (P_{1i} - P_{2i}) - \frac{V_{02i} - A_{2i} d_i}{\beta_e} \dot{P}_{2i} = Q_{2i} \end{cases} \quad (30)$$

where A_{1i} and A_{2i} denote the ram areas of the two cylinder chambers, C_{ii} is the coefficient of the internal leakage of the cylinder, β_e is the effective bulk modulus, and V_{01i} and V_{02i} are the original total control volumes of the cylinder chambers.

According to Fig. 6, the cylinder dynamics can be described by

$$A_{1i} P_{1i} - A_{2i} P_{2i} = f_i + f_{friction} = f_i + F_{ci} \text{sgn}(\dot{d}_i) + \beta_i \dot{d}_i \quad (31)$$

where f_i , defined in Equation (15), is the driving force on the piston of the cylinder; $f_{friction}$ is the equivalent friction force; \dot{d}_i is the velocity of the pairs of cylinders; β_i is the viscous friction coefficient; and F_{ci} is the Coulomb friction.

Neglecting the servo-valve dynamics due to the low working frequency, the control applied to the valve can be approximately proportional to the valve spool position. Thus,

$$x_{vi} = k_{vi} u_i. \quad (32)$$

The state variables are defined as

$z = [z_1 \ z_2 \ z_3 \ z_4 \ z_5 \ z_6 \ z_7 \ z_8]^T$, where $z_1 = d_1$, $z_2 = \dot{d}_1$, $z_3 = P_{11}$, $z_4 = P_{21}$, $z_5 = d_2$, $z_6 = \dot{d}_2$, $z_7 = P_{12}$, and $z_8 = P_{22}$. Combining Equations (15), (27), (30), and (31) leads to

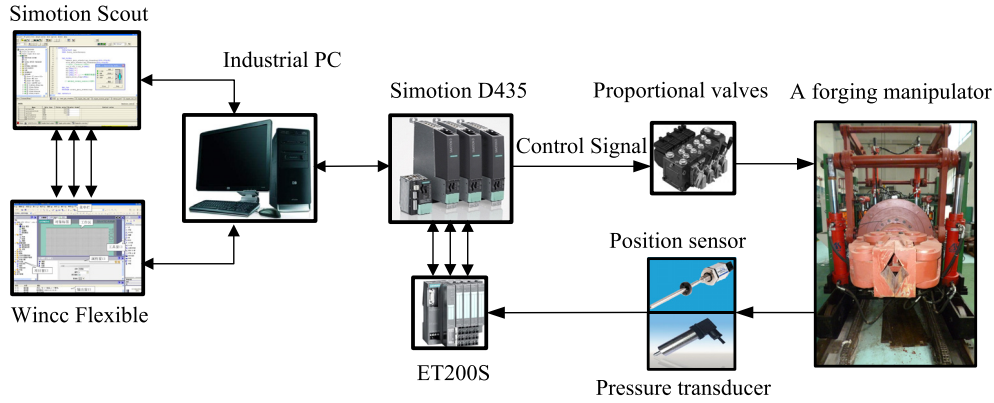


FIGURE 7. Control system diagram of the experimental forging manipulator.

the state space representation of the main motion system with the multi-closed-loop mechanism as follows:

$$\begin{cases} \dot{z}_1 = z_2 \\ \dot{z}_5 = z_6 \\ \begin{bmatrix} \dot{z}_2 \\ \dot{z}_6 \end{bmatrix} = [D(z_1, z_5)]^{-1} \begin{bmatrix} A_{11}z_3 - A_{21}z_4 \\ A_{12}z_7 - A_{22}z_8 \end{bmatrix} - F_e(z) \\ \dot{z}_3 = h_1(z) + g_1(z, u_1) \\ \dot{z}_4 = h_2(z) + g_2(z, u_1) \\ \dot{z}_7 = h_3(z) + g_3(z, u_2) \\ \dot{z}_8 = h_4(z) + g_4(z, u_2) \\ y = [z_1 \quad z_5]^T \end{cases} \quad (33)$$

where

$$F_e(z) = C(z_1, z_2, z_5, z_6) [z_2 \quad z_6]^T + G(z_1, z_5) + f_{friction}(z_2, z_6)$$

is a two-dimensional vector; $C(z_1, z_2, z_5, z_6)$, $G(z_1, z_5)$, and $D(z_1, z_5)$ are defined in Equation (15);

$$\begin{aligned} h_1(z) &= \beta_e [-A_{11}z_2 - C_{t1} (z_3 - z_4)] / (V_{011} + A_{11}z_1); \\ h_2(z) &= \beta_e [A_{21}z_2 + C_{t1} (z_3 - z_4)] / (V_{021} - A_{21}z_1); \\ h_3(z) &= \beta_e [-A_{12}z_6 - C_{t2} (z_7 - z_8)] / (V_{012} + A_{12}z_5); \\ h_4(z) &= \beta_e [A_{22}z_6 + C_{t2} (z_7 - z_8)] / (V_{022} - A_{22}z_5); \\ g_1(z, u_1) &= \beta_e Q_{11}(z, u_1) / (V_{011} + A_{11}z_1); \\ g_2(z, u_1) &= -\beta_e Q_{21}(z, u_1) / (V_{021} - A_{21}z_1); \\ g_3(z, u_2) &= \beta_e Q_{12}(z, u_2) / (V_{012} + A_{12}z_5); \\ g_4(z, u_2) &= -\beta_e Q_{22}(z, u_2) / (V_{022} - A_{22}z_5); \end{aligned}$$

y is the output vector of the hydraulic robotic manipulator.

Equation (33) represents the derived closed-form dynamic system for the main motion system with multi-closed-loop mechanisms by considering the dynamics of the hydraulic actuators. As the output of the model is explicit with respect to the system inputs, that is, the valve spool position of practical hydraulic cylinders, the model is ready to be used in system dynamics analysis and controller design.

V. MODEL VALIDATION AND EXPERIMENTS

A. EXPERIMENT SETUP

The system dynamic model is tested on an experimental forging manipulator that is designed and built in the School of Mechanical and Electrical Engineering at Central South University in China [8]. The schematic of its control system is shown in Fig. 7. The manipulator is driven by three pairs of symmetrically arranged hydraulic cylinders. The proportional flow control valves are PVG32 valves (made by American Sauer Danfoss Company). An industrial motion controller: SIMOTION D435 (industrial motion control system from Siemens automation, Inc.) is applied as physical hardware to control the hydraulic cylinders. The distributed I/O data acquisition component: ET200S (distributed I/O system from Siemens automation, Inc.) is used to communicate with external sensors (to measure positions and pressures). The SIMOTION motion control software is Simotion Scout, which can achieve configuration, programming, testing or commissioning, and runtime functionality. Human-interactive and data acquisition programs are written by Wincc flexible software. In the experiment, pitching cylinders are locked. The mathematical model is validated in the experimental forging manipulator.

B. MODEL PARAMETER IDENTIFICATION

The parameters of the dynamic model can be determined by parameter identification techniques and certain physical experiments. For example, the mass, length, and moment of inertia of the linkages can be measured by three-dimensional modeling software, such as Solidworks, PROE, and CATIA because the structure of the manipulator is designed and built by our research team. The parameters of the linkages are given in detail in [8]. Parameters V_{01i} , V_{02i} , and C_{ti} in Equation (30) can be identified using the nonlinear optimization function *fmincon* in MATLAB software after obtaining the state values from sensors. Similarly, friction parameters F_{ci} and β_i in Equation (31) can be identified after obtaining the linkage parameters and the system's state values. Other

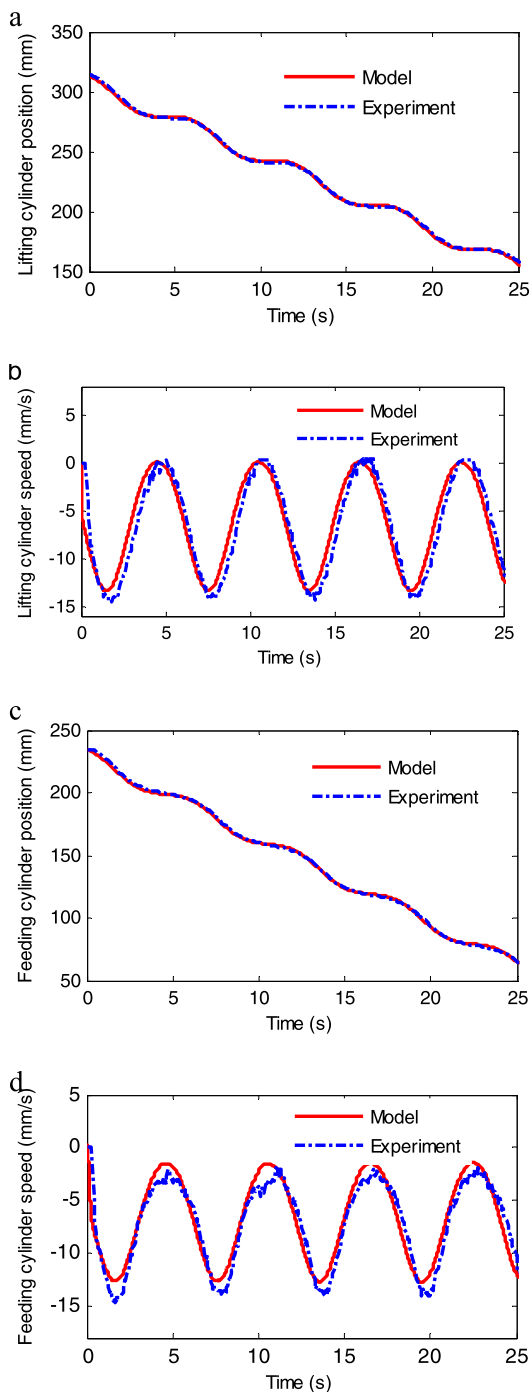


FIGURE 8. Comparison between the mathematical model and the physical experimental system.

parameters can be obtained from the manufacturer’s technical documents.

C. MODEL VALIDATION

Pitching hydraulic cylinders are fixed, and the gripper remains horizontal during the experiments. Two sinusoidal signals, $u_1 = -(0.5 \sin(\pi t/3) + 3.8)$ and $u_2 = -(0.35 \sin(\pi t/3) + 2.3)$, are inputted to the two control proportional valves of the lifting and horizontal feeding hydraulic cylinders by the motion controller. The two

sinusoidal signals are taken as the inputs of the established closed-form dynamic model for the main motion system of the forging manipulator. Note that the velocity and acceleration signals are estimated by a Kalman observer to avoid amplifying the sensor noise in the numerical calculation [49], [50]. The comparisons between the outputs of the mathematical model and experiments are shown in Fig. 8. From Figs. 8(a), (b), (c), and (d), the mathematical model (described by Equation (33)) of the system can capture the relevant trends of the hydraulic robotic manipulator with a maximum error of 12%. This result may be due to the uncertainties of the hydraulic system. Another observation is a lag between the velocity outputs of the model and the measurement. Two possible reasons can explain the lag. One may be the measurement lag of the position sensor in the digital system with a sampling period of 57 ms. The other may be because of the velocity estimation lag from using the Kalman observer.

VI. CONCLUSIONS

The systematic application of the reduced system dynamic method in combination with Lagrangian formulation, the principle of virtual work and screw theory is presented to establish explicit control-orientated closed-form dynamic equations for the main motion system of a heavy-duty hydraulic manipulator with multi-closed-loop mechanisms. By analyzing the motion characteristic of the main motion system, the dynamic equations of motion for the main motion system with only three simple coupled subsystems, two Jacobian matrices, and two Hessian matrices are obtained, which greatly reduces the complexity of closed-form dynamic equations. The Jacobian and Hessian matrices are straightforwardly calculated by screw theory, simplifying the calculation of the two Hessian matrices and making closed-form dynamic equations concise. No parts of dynamic equations are neglected in the derivation of the dynamic model. Thus, the derived dynamic equations for the main motion system are accurate and obtained in a simple manner. To the best knowledge of the authors, combining the reduced system dynamic method with Lagrangian formulation and the principle of virtual work with a straightforward calculation of the Hessian matrices by screw theory has not been considered in previous works. Such calculation can establish the concise dynamics of the complex multi-closed-loop mechanisms. By adding the dynamics of the hydraulic cylinders, the derived closed-form system model for the main motion system with multi-closed-loop mechanisms is explicit with respect to the system inputs, that is, the valve spool position of the practical hydraulic cylinders. Hence, its dynamic response can be obtained in the most direct manner. Thus, the concise, computational efficient, and explicit closed-form dynamic equations are systematically established for the main motion system, which can facilitate dynamics analysis and controller design. The efficiency of the proposed approach is illustrated with the experiments on the main motion system of a heavy-duty hydraulic forging manipulator.

No systematic approach that divides a complex multi-closed-loop mechanism into simple subchains is available for the reduced system dynamic method. Accordingly, one of our future work is to study the manner in which a complex multi-closed-loop mechanism can be optimally decomposed into the least number of subchains.

APPENDIX

A. THE ELEMENTS OF DYNAMIC EQUATIONS FOR THE MULTI-CLOSED-LOOP ROBOT MECHANICAL SYSTEM

$$\begin{aligned}
 \mathbf{M}_1(\mathbf{q}) &= \begin{bmatrix} M_{111} & M_{112} \\ M_{121} & M_{122} \end{bmatrix}; \\
 \mathbf{C}_1(\mathbf{q}, \dot{\mathbf{q}}) &= \begin{bmatrix} C_{111} & C_{112} \\ C_{121} & C_{122} \end{bmatrix}; \\
 \mathbf{G}_1(\mathbf{q}) &= \begin{bmatrix} G_{111} \\ G_{121} \end{bmatrix}; \\
 M_{111} &= \begin{bmatrix} m_1 r_1^2 + m_2 r_2^2 + m_3 l_5^2 + I_{C_1} + I_{C_2} + I_{C_4} \\ + m_4 (l_1^2 + 2l_1 r_4 \cos \theta_2 + r_4^2) \\ + m_5 (l_1^2 + 2l_1 l_2 \cos \theta_2 + l_2^2) \\ + m_7 (l_1^2 + 2l_1 r_7 \cos \theta_2 + r_7^2) + I_{C_7} \end{bmatrix}; \\
 M_{112} &= M_{121} \\
 &= m_4 (l_1 r_4 \cos \theta_2 + r_4^2) + m_5 (l_1 l_2 \cos \theta_2 + l_2^2) \\
 &\quad + m_7 (l_1 r_7 \cos \theta_2 + r_7^2) + I_{C_4} + I_{C_7} \\
 M_{122} &= m_4 r_4^2 + m_5 l_2^2 + m_7 r_7^2 + I_{C_4} + I_{C_7}; \\
 C_{111} &= -2m_7 l_1 r_7 \dot{\theta}_2 \sin \theta_2 - 2m_4 l_1 r_4 \dot{\theta}_2 \sin \theta_2 \\
 &\quad - 2m_5 l_1 l_2 \dot{\theta}_2 \sin \theta_2; \\
 C_{112} &= -m_7 l_1 r_7 \dot{\theta}_2 \sin \theta_2 - m_4 l_1 r_4 \dot{\theta}_2 \sin \theta_2 \\
 &\quad - m_5 l_1 l_2 \dot{\theta}_2 \sin \theta_2; \\
 C_{121} &= m_7 l_1 r_7 \dot{\theta}_1 \sin \theta_2 + m_4 l_1 r_4 \dot{\theta}_1 \sin \theta_2 \\
 &\quad + m_5 l_1 l_2 \dot{\theta}_1 \sin \theta_2; \\
 C_{122} &= 0; \\
 G_{111} &= \begin{bmatrix} -m_1 g r_1 \cos(\theta_1 + \phi_1) - m_4 g (l_1 \cos \theta_1 \\ + r_4 \cos(\theta_1 + \theta_2)) \\ -m_5 g (l_1 \cos \theta_1 + l_2 \cos(\theta_1 + \theta_2)) \\ -m_7 g (l_1 \cos \theta_1 + r_7 \cos(\theta_1 + \theta_2)) \\ -m_2 g r_2 \cos(\theta_1 + \phi_2) \\ -m_3 g l_5 \cos(\theta_1 + \phi_4) \end{bmatrix}; \\
 G_{121} &= -m_4 g r_4 \cos(\theta_1 + \theta_2) - m_5 g l_2 \cos(\theta_1 + \theta_2) \\
 &\quad - m_7 g r_7 \cos(\theta_1 + \theta_2) \\
 \mathbf{D}_2(\mathbf{q}_2) &= \begin{bmatrix} D_{211} & D_{212} \\ D_{221} & D_{222} \end{bmatrix}; \\
 \mathbf{H}_{C_2}(\mathbf{q}_2) &= \begin{bmatrix} \begin{pmatrix} H_{C_{2111}} \\ H_{C_{2112}} \end{pmatrix} & \begin{pmatrix} H_{C_{2121}} \\ H_{C_{2122}} \end{pmatrix} \\ \begin{pmatrix} H_{C_{2211}} \\ H_{C_{2212}} \end{pmatrix} & \begin{pmatrix} H_{C_{2221}} \\ H_{C_{2222}} \end{pmatrix} \end{bmatrix}; \\
 \mathbf{g}_2(\mathbf{q}_2) &= \begin{bmatrix} g_{21} \\ g_{22} \end{bmatrix}; \\
 D_{211} &= m_8 r_8^2 + I_{C_8} + I_{C_9} + m_9 (d_1 - r_9)^2; \\
 D_{212} &= D_{221} = 0; \quad D_{222} = m_9; \\
 H_{C_{2111}} &= 0; \quad H_{C_{2112}} = 2m_9 (d_1 - r_9);
 \end{aligned}$$

$$\begin{aligned}
 H_{C_{2121}} &= H_{C_{2122}} = 0; \\
 H_{C_{2211}} &= -m_9 (d_1 - r_9); \\
 H_{C_{2212}} &= H_{C_{2221}} = H_{C_{2222}} = 0; \\
 g_{21} &= m_8 g r_8 \cos \theta_4 + m_9 g (d_1 - r_9) \cos \theta_4; \\
 g_{22} &= m_9 g \sin \theta_4; \\
 \mathbf{D}_3(\mathbf{q}_3) &= \begin{bmatrix} D_{311} & D_{312} \\ D_{321} & D_{322} \end{bmatrix}; \\
 \mathbf{H}_{C_3}(\mathbf{q}_3) &= \begin{bmatrix} \begin{pmatrix} H_{C_{3111}} \\ H_{C_{3112}} \end{pmatrix} & \begin{pmatrix} H_{C_{3121}} \\ H_{C_{3122}} \end{pmatrix} \\ \begin{pmatrix} H_{C_{3211}} \\ H_{C_{3212}} \end{pmatrix} & \begin{pmatrix} H_{C_{3221}} \\ H_{C_{3222}} \end{pmatrix} \end{bmatrix}; \\
 \mathbf{g}_3(\mathbf{q}_3) &= \begin{bmatrix} g_{31} \\ g_{32} \end{bmatrix}; \\
 D_{311} &= m_{10} r_{10}^2 + I_{C_{10}} + I_{C_{11}} + m_{11} (d_2 - r_{11})^2; \\
 D_{312} &= D_{321} = 0; \quad D_{322} = m_{11}; \\
 H_{C_{3111}} &= 0; \quad H_{C_{3112}} = 2m_{11} (d_2 - r_{11}); \\
 H_{C_{3121}} &= H_{C_{3122}} = 0; \\
 H_{C_{3211}} &= -m_{11} (d_2 - r_{11}); \quad H_{C_{3212}} = H_{C_{3221}} = H_{C_{3222}} = 0; \\
 g_{31} &= -m_{10} g r_{10} \cos \theta_5 - m_{11} g (d_2 - r_{11}) \cos \theta_5; \\
 g_{32} &= -m_{11} g \sin \theta_5;
 \end{aligned}$$

where m_i denotes the mass of link i ($i = 1, 2, 3 \dots 11$); l_i denotes the length of link i ($i = 1, 2 \dots, 6$); r_i denotes the distance from the previous joint to the center of mass of link i ; I_{C_i} denotes the moment of inertia of link i .

B. ELEMENTS OF THE MATRICES $J_3^{(1)}$, $H_3^{(1)}$, $J_3^{(3)}$ and $H_3^{(3)}$

$$\begin{aligned}
 \mathbf{J}_3^{(1)} &= \begin{bmatrix} s_G \times (P_E - R_G) & s_F \times (P_E - R_F) \end{bmatrix}; \\
 \mathbf{H}_3^{(1)} &= \begin{bmatrix} s_G \times [s_G \times (P_E - R_G)] & s_G \times [s_F \times (P_E - R_F)] \\ s_G \times [s_F \times (P_E - R_F)] & s_F \times [s_F \times (P_E - R_F)] \\ 0 & 0 \end{bmatrix}; \\
 \mathbf{J}_3^{(3)} &= \begin{bmatrix} s_L \times (P_E - R_L) & s_{LE} \end{bmatrix}; \\
 \mathbf{H}_3^{(3)} &= \begin{bmatrix} s_L \times [s_L \times (P_E - R_L)] & s_L \times s_{LE} \\ s_L \times s_{LE} & 0 \\ 0 & 0 \end{bmatrix}.
 \end{aligned}$$

C. ELEMENTS OF THE MATRICES J_i AND H_i

$$\begin{aligned}
 \mathbf{J}_2(\mathbf{q}_2, \mathbf{q}) &= \begin{bmatrix} J_{211} & J_{212} \\ J_{221} & J_{222} \end{bmatrix} \\
 \mathbf{J}_3(\mathbf{q}_3, \mathbf{q}) &= \begin{bmatrix} J_{311} & J_{312} \\ J_{321} & J_{322} \end{bmatrix} \\
 \mathbf{J}(\mathbf{q}, \mathbf{d}) &= \begin{bmatrix} J_{11} & J_{12} \\ J_{21} & J_{22} \end{bmatrix} \\
 J_{211} &= -l_6 \cos(\theta_4 + \theta_1 + \varphi_5) / d_1; \\
 J_{212} &= 0; \\
 J_{221} &= -l_6 \sin(\theta_4 + \theta_1 + \varphi_5); \\
 J_{222} &= 0 \\
 J_{311} &= [l_1 \cos(-\theta_5 + \theta_1) + l_4 \cos(-\theta_5 + \theta_1 + \theta_2)] / d_2; \\
 J_{312} &= [l_4 \cos(-\theta_5 + \theta_1 + \theta_2)] / d_2
 \end{aligned}$$

$$J_{321} = -l_1 \sin(-\theta_5 + \theta_1) - l_4 \sin(-\theta_5 + \theta_1 + \theta_2);$$

$$J_{322} = -l_4 \sin(-\theta_5 + \theta_1 + \theta_2)$$

$$J_{11} = l_6 y_Q \cos(\theta_1 + \varphi_5) + l_6 z_Q \sin(\theta_1 + \varphi_5)/d_1;$$

$$J_{12} = 0;$$

$$J_{21} = y_L l_1 \cos \theta_1 + y_L l_4 \cos(\theta_1 + \theta_2) + z_L l_1 \sin \theta_1 + z_L l_4 \sin(\theta_1 + \theta_2)/d_2;$$

$$J_{22} = l_4 [y_L \cos(\theta_1 + \theta_2) + z_L \sin(\theta_1 + \theta_2) - l_1 \sin \theta_2]/d_2;$$

$$H_2(q_2, q) = \begin{bmatrix} \begin{pmatrix} H_{2111} \\ H_{2112} \\ H_{2211} \\ H_{2212} \end{pmatrix} & \begin{pmatrix} H_{2121} \\ H_{2122} \\ H_{2221} \\ H_{2222} \end{pmatrix} \end{bmatrix};$$

$$H_3(q_3, q) = \begin{bmatrix} \begin{pmatrix} H_{3111} \\ H_{3112} \\ H_{3211} \\ H_{3212} \end{pmatrix} & \begin{pmatrix} H_{3121} \\ H_{3122} \\ H_{3221} \\ H_{3222} \end{pmatrix} \end{bmatrix};$$

$$H_{2111} = l_6 \sin(\theta_4 + \theta_1 + \varphi_5) \times [-2l_6 \cos(\theta_4 + \theta_1 + \varphi_5) + d_1]/d_1^2;$$

$$H_{2211} = l_6 \cos(\theta_4 + \theta_1 + \varphi_5) \times [l_6 \cos(\theta_4 + \theta_1 + \varphi_5) - d_1]/d_1;$$

$$H_{2112} = H_{2121} = H_{2122} = H_{2212} = H_{2221} = H_{2222} = 0;$$

$$H_{3111} = \frac{1}{d_2^2} \begin{bmatrix} l_1^2 \sin(-2\theta_5 + 2\theta_1) \\ + 2l_1 l_4 \sin(-2\theta_5 + 2\theta_1 + \theta_2) \\ + l_4^2 \sin(-2\theta_5 + 2\theta_1 + 2\theta_2) \\ - l_1 d_2 \sin(-\theta_5 + \theta_1) \\ - l_4 d_2 \sin(-\theta_5 + \theta_1 + \theta_2) \end{bmatrix};$$

$$H_{3112} = \begin{bmatrix} l_1 l_4 \sin(-2\theta_5 + 2\theta_1 + \theta_2) \\ + l_4^2 \sin(-2\theta_5 + 2\theta_1 + 2\theta_2) \\ - l_4 d_2 \sin(-\theta_5 + \theta_1 + \theta_2) \end{bmatrix} / d_2^2;$$

$$H_{3121} = \begin{bmatrix} l_1 l_4 \sin(-2\theta_5 + 2\theta_1 + \theta_2) \\ + l_4^2 \sin(-2\theta_5 + 2\theta_1 + 2\theta_2) \\ - l_4 d_2 \sin(-\theta_5 + \theta_1 + \theta_2) \end{bmatrix} / d_2^2;$$

$$H_{3122} = \begin{bmatrix} l_4^2 \sin(-2\theta_5 + 2\theta_1 + 2\theta_2) \\ - l_4 d_2 \sin(-\theta_5 + \theta_1 + \theta_2) \end{bmatrix} / d_2^2;$$

$$H_{3211} = * [l_1 \cos(-\theta_5 + \theta_1) + l_4 \cos(-\theta_5 + \theta_1 + \theta_2)] / d_2;$$

$$H_{3212} = * [l_1 \cos(-\theta_5 + \theta_1) + l_4 \cos(-\theta_5 + \theta_1 + \theta_2) - d_2] / d_2;$$

$$H_{3221} = * [l_1 \cos(-\theta_5 + \theta_1) + l_4 \cos(-\theta_5 + \theta_1 + \theta_2) - d_2] / d_2;$$

$$H_{3222} = l_4 \cos(-\theta_5 + \theta_1 + \theta_2) \times [l_4 \cos(-\theta_5 + \theta_1 + \theta_2) - d_2] / d_2.$$

REFERENCES

[1] Z. Wang, N. Zhang, X. Chai, and Q. Li, "Kinematic/dynamic analysis and optimization of a 2-URR-RRU parallel manipulator," *Nonlinear Dyn.*, vol. 88, no. 1, pp. 503–519, Apr. 2017.

[2] M. Gabardi, M. Solazzi, and A. Frisoli, "An optimization procedure based on kinematics analysis for the design parameters of a 4-UPU parallel manipulator," *Mechanism Mach. Theory*, vol. 133, pp. 211–228, Mar. 2019.

[3] T. Sun and S. Yang, "An approach to formulate the hessian matrix for dynamic control of parallel robots," *IEEE/ASME Trans. Mechatronics*, vol. 24, no. 1, pp. 271–281, Feb. 2019.

[4] D. Chablat and P. Wenger, "Architecture optimization of a 3-DOF translational parallel mechanism for machining applications, the orthoglide," *IEEE Trans. Robot. Autom.*, vol. 19, no. 3, pp. 403–410, Jun. 2003.

[5] M. Diaz-Rodriguez, A. Valera, V. Mata, and M. Valles, "Model-based control of a 3-DOF parallel robot based on identified relevant parameters," *IEEE/ASME Trans. Mechatronics*, vol. 18, no. 6, pp. 1737–1744, Dec. 2013.

[6] J. Yoon, J. Kim, J. Seo, and S. Suh, "Spatial factors affecting the loading efficiency of excavators," *Autom. Construct.*, vol. 48, pp. 97–106, Dec. 2014.

[7] N. Luan, H. Zhang, and S. Tong, "Optimum motion control of palletizing robots based on iterative learning," *Ind. Robot, Int. J.*, vol. 39, no. 2, pp. 162–168, Mar. 2012.

[8] W.-H. Ding, H. Deng, Q.-M. Li, and Y.-M. Xia, "Control-orientated dynamic modeling of forging manipulators with multi-closed kinematic chains," *Robot. Comput.-Integr. Manuf.*, vol. 30, no. 5, pp. 421–431, Oct. 2014.

[9] S. Staicu and D. Zhang, "A novel dynamic modelling approach for parallel mechanisms analysis," *Robot. Comput.-Integr. Manuf.*, vol. 24, no. 1, pp. 167–172, Feb. 2008.

[10] P.-L. Yen and C.-C. Lai, "Dynamic modeling and control of a 3-DOF Cartesian parallel manipulator," *Mechatronics*, vol. 19, no. 3, pp. 390–398, Apr. 2009.

[11] B. Han, D. Zheng, Y. Xu, J. Yao, and Y. Zhao, "Kinematic characteristics and dynamics analysis of an overconstrained scissors double-hoop truss deployable antenna mechanism based on screw theory," *IEEE Access*, vol. 7, pp. 140755–140768, 2019.

[12] Z. Liao, L. Yao, Z. Lu, and J. Zhang, "Screw theory based mathematical modeling and kinematic analysis of a novel ankle rehabilitation robot with a constrained 3-PSP mechanism topology," *Int. J. Intell. Robot. Appl.*, vol. 2, no. 3, pp. 351–360, Sep. 2018.

[13] J. Gallardo-Alvarado, M. H. Abedinnasab, and M. N. Islam, "A simple method to solve the instantaneous kinematics of the 5-RUR parallel manipulator," *Robotica*, vol. 37, no. 6, pp. 1143–1157, Jun. 2019.

[14] G. Cheng and X. Shan, "Dynamics analysis of a parallel hip joint simulator with four degree of freedoms (3R1T)," *Nonlinear Dyn.*, vol. 70, no. 4, pp. 2475–2486, Dec. 2012.

[15] G. Xin, H. Deng, and G. Zhong, "Closed-form dynamics of a 3-DOF spatial parallel manipulator by combining the lagrangian formulation with the virtual work principle," *Nonlinear Dyn.*, vol. 86, no. 2, pp. 1329–1347, Oct. 2016.

[16] Z. Wang and F. H. Ghorbel, "Control of closed kinematic chains: A comparative study," in *Proc. Amer. Control Conf.*, Minneapolis, MN, USA, Jun. 2006, p. 6.

[17] W.-H. Ding, H. Deng, Y.-M. Xia, and X.-G. Duan, "Tracking control of electro-hydraulic servo multi-closed-chain mechanisms with the use of an approximate nonlinear internal model," *Control Eng. Pract.*, vol. 58, pp. 225–241, Jan. 2017.

[18] B. Dasgupta and T. S. Mruthyunjaya, "Closed-form dynamic equations of the general stewart platform through the Newton–Euler approach," *Mechanism Mach. Theory*, vol. 33, no. 7, pp. 993–1012, Oct. 1998.

[19] R. F. Abo-Shanab, "Dynamic modeling of parallel manipulators based on Lagrange–D'Alembert formulation and Jacobian/Hessian matrices," *Multibody Syst. Dyn.*, vol. 48, no. 4, pp. 403–426, Apr. 2020.

[20] A. M. Shafei and H. R. Shafei, "Dynamic modeling of planar closed-chain robotic manipulators in flight and impact phases," *Mechanism Mach. Theory*, vol. 126, pp. 141–154, Aug. 2018.

[21] Y. Han, "Kane method based dynamics modeling and control study for space manipulator capturing a space target," *Int. J. Aerosp. Eng.*, vol. 2016, Jul. 2016, Art. no. 7375685.

[22] T. W. Tu, "First-order form, Lagrange's form, and Gibbs–Appell's form of Kane's equations," *Acta Mechanica* vol. 227, pp. 1885–1901, Apr. 2016.

[23] M. H. Korayem, A. M. Shafei, and S. F. Dehkordi, "Systematic modeling of a chain of N-flexible link manipulators connected by revolute-prismatic joints using recursive Gibbs–Appell formulation," *Arch. Appl. Mech.*, vol. 84, no. 2, pp. 187–206, Feb. 2014.

- [24] V. Mata, S. Provenzano, F. Valero, and J. I. Cuadrado, "Serial-robot dynamics algorithms for moderately large numbers of joints," *Mechanism Mach. Theory*, vol. 37, no. 8, pp. 739–755, Aug. 2002.
- [25] A. M. Shafei and H. R. Shafei, "A systematic method for the hybrid dynamic modeling of open kinematic chains confined in a closed environment," *Multibody Syst. Dyn.*, vol. 38, no. 1, pp. 21–42, Sep. 2016.
- [26] M. H. Korayem and S. F. Dehkordi, "Dynamic modeling of flexible cooperative mobile manipulator with revolute-prismatic joints for the purpose of moving common object with closed kinematic chain using the recursive Gibbs–Appell formulation," *Mechanism Mach. Theory*, vol. 137, pp. 254–279, Jul. 2019.
- [27] H. Kalani, A. Rezaei, and A. Akbarzadeh, "Improved general solution for the dynamic modeling of Gough–Stewart platform based on principle of virtual work," *Nonlinear Dyn.*, vol. 83, no. 4, pp. 2393–2418, Mar. 2016.
- [28] X. Yuan and J. Zhu, "Inverse dynamic modeling and analysis of a coaxial helicopter's swashplate mechanism," *Mechanism Mach. Theory*, vol. 113, pp. 208–230, Jul. 2017.
- [29] J. Gallardo-Alvarado, R. Rodríguez-Castro, and P. J. Delossantos-Lara, "Kinematics and dynamics of a 4-PRUR Schönflies parallel manipulator by means of screw theory and the principle of virtual work," *Mechanism Mach. Theory*, vol. 122, pp. 347–360, Apr. 2018.
- [30] H. B. Guo and H. Li, "Dynamic analysis and simulation of a six degree of freedom Stewart platform manipulator," in *Proc. Inst. Mech. Eng., C, J. Mech. Eng. Sci.*, vol. 220, pp. 61–72, Jan. 2006.
- [31] H. G. Sage, M. F. De Mathelin, and E. Ostertag, "Robust control of robot manipulators: A survey," *Int. J. Control*, vol. 72, no. 16, pp. 1498–1522, Jan. 1999.
- [32] F. H. Ghorbel, O. Chetelat, R. Gunawardana, and R. Longchamp, "Modeling and set point control of closed-chain mechanisms: Theory and experiment," *IEEE Trans. Control Syst. Technol.*, vol. 8, no. 5, pp. 801–815, Sep. 2000.
- [33] R. Kelly, "PD control with desired gravity compensation of robotic manipulators: A review," *Int. J. Robot. Res.*, vol. 16, no. 5, pp. 660–672, Oct. 1997.
- [34] A. Zavala-Rio and V. Santibanez, "A natural saturating extension of the PD-with-desired-gravity-compensation control law for robot manipulators with bounded inputs," *IEEE Trans. Robot.*, vol. 23, no. 2, pp. 386–391, Apr. 2007.
- [35] H. Cheng, Y.-K. Yiu, and Z. Li, "Dynamics and control of redundantly actuated parallel manipulators," *IEEE/ASME Trans. Mechatronics*, vol. 8, no. 4, pp. 483–491, Dec. 2003.
- [36] S.-H. Hsu and L.-C. Fu, "A fully adaptive decentralized control of robot manipulators," *Automatica*, vol. 42, no. 10, pp. 1761–1767, Oct. 2006.
- [37] S.-H. Lee, J.-B. Song, W.-C. Choi, and D. Hong, "Position control of a stewart platform using inverse dynamics control with approximate dynamics," *Mechatronics*, vol. 13, no. 6, pp. 605–619, Jul. 2003.
- [38] J. Wittenburg, *Dynamics of Systems of Rigid Bodies*. Brunswick, German: Springer-Verlag, 1977.
- [39] J. Gallardo, J. M. Rico, A. Frisoli, D. Checcacci, and M. Bergamasco, "Dynamics of parallel manipulators by means of screw theory," *Mechanism Mach. Theory*, vol. 38, no. 11, pp. 1113–1131, Nov. 2003.
- [40] J. Gallardo-Alvarado and J. M. Rico-Martinez, "Jerk influence coefficients, via screw theory, of closed chains," *Meccanica*, vol. 36, no. 2, pp. 213–228, Mar. 2001.
- [41] A. Cibicik and O. Egeland, "Dynamic modelling and force analysis of a knuckle boom crane using screw theory," *Mechanism Mach. Theory*, vol. 133, pp. 179–194, Mar. 2019.
- [42] S. Li, N. Ma, and W. Ding, "Kinematic analysis of a novel 3-DOF 3-RPUR translational parallel mechanism," in *Proc. IEEE/ASME Int. Conf. AIM*, Xian, China, Jul. 2008, pp. 516–521.
- [43] S. J. Zhu, Z. Huang, and H. F. Ding, "Forward/Reverse velocity and acceleration analysis for a class of lower-mobility parallel mechanisms," *J. Mech. Des.*, vol. 129, no. 4, pp. 390–396, Apr. 2007.
- [44] Z. Huang, Y.-S. Zhao, and T.-S. Zhao, *Advanced Spatial Mechanism*, 2nd ed. Beijing, China: High Education Press (in Chinese), 2014.
- [45] D. Wu, R. Burton, G. Schoenau, and D. Bitner, "Analysis of a pressure-compensated flow control valve," *J. Dyn. Syst., Meas., Control*, vol. 129, no. 2, pp. 203–211, Mar. 2007.
- [46] C. Guan and S. Pan, "Nonlinear adaptive robust control of single-rod electro-hydraulic actuator with unknown nonlinear parameters," *IEEE Trans. Control Syst. Technol.*, vol. 16, no. 3, pp. 434–445, May 2008.
- [47] C.-Y. Chen, L.-Q. Liu, C.-C. Cheng, and G. T.-C. Chiu, "Fuzzy controller design for synchronous motion in a dual-cylinder electro-hydraulic system," *Control Eng. Pract.*, vol. 16, no. 6, pp. 658–673, Jun. 2008.
- [48] S. Liu and B. Yao, "Automated onboard modeling of cartridge valve flow mapping," *IEEE/ASME Trans. Mechatronics*, vol. 11, no. 4, pp. 381–388, Aug. 2006.
- [49] D. Kostic, B. D. Jager, M. Steinbuch, and R. Hensen, "Modeling and identification for high-performance robot control: An RRR-robotic arm case study," *IEEE Trans. Control Syst. Technol.*, vol. 12, no. 6, pp. 904–919, Nov. 2004.
- [50] P. R. Belanger, "Estimation of angular velocity and acceleration from shaft encoder measurements," in *Proc. IEEE ICRA*, Nice, France, May 1992, pp. 585–592.



YI ZHANG received the B.E. and Ph.D. degrees from the School of Mechanical and Electrical Engineering, Central South University, China. He is currently a Postdoctoral Fellow with the School of Mechanical and Electrical Engineering, Central South University. He is also a Lecturer with the School of Mechanical and Electrical Engineering, Changsha University, China. His current research interests include mechanism design, and system modeling and control.



WENHUA DING received the Ph.D. degree in mechanical engineering from Central South University, China, in 2015. He is currently a Robot Product Manager of Shenzhen Colibri Technologies Company Ltd., China. He is mainly engaged in the research and development of robots and motion control products.



HUA DENG (Member, IEEE) received the B.E. degree in electrical engineering from the Nanjing Aeronautical Institute, Nanjing, China, in 1983, the M.E. degree in electrical engineering from Northwestern Polytechnical University, Xi'an, China, in 1988, and the Ph.D. degree in manufacturing engineering from the City University of Hong Kong, Kowloon, Hong Kong, in 2005. He is currently a Professor with the School of Mechanical and Electrical Engineering, Central South University, Changsha, China. His research interests include intelligent control and learning, robotic dynamics and control, biomechanics, and modeling and control of complex distributed parameter systems.

...